OPTICAL MODEL PARAMETERS FROM AVERAGE TOTAL NEUTRON CROSS SECTIONS

by

Robert Henry Tabony

Department of Physics
Duke University

Date: April 11, 1966

Approved:

Henry W. Newson, Chairman

A dissertation submitted in partial fulfillment of the requirements for the degree of Doctor of Philosophy in the Department of Physics in the Graduate School of Arts and Sciences of Duke University

1966

ABSTRACT

OPTICAL MODEL PARAMETERS FROM AVERAGE TOTAL NEUTRON CROSS SECTIONS

by

Robert Henry Tabony
Department of Physics
Duke University

Date: April 11, 1966

Approved:

Henry W. Newson

Henry W. Newson, Chairman

A. Hashizume

Harold W. Lewis

D. R. Tilley

J. D. Bussel

An abstract of a dissertation submitted in partial fulfillment of the requirements for the degree of Doctor of Philosophy in the Department of Physics in the Graduate School of Arts and Sciences of Duke University

1966

ABSTRACT

Neutron total cross sections of Ru, In, Sb, I, La, Hf, Ta, W, Re, Os, Ir, Hg, Th, and U have been measured in the energy region from 30 kev to 650 kev. A number of different sample thicknesses were used for each element, and the transmission data was analyzed for s-, p-, and d-wave strength functions and shape-elastic scattering phase shifts by area methods, modified to include the effects of Doppler broadening and the Porter Thomas distribution function for neutron reduced widths. The important results include the verification of the splitting of both the s-wave strength function peak and the shape-elastic phase-shift peak due to the deformation of nuclei in the neighborhood of A = 170. The broad minimum in the p-wave strength function in the region A = 120 - 190 as well as the rather large d-wave strength function in the region A = 120 to 190 are also observed. The results are interpreted in terms of the optical model.

ACKNOWLEDGEMENTS

I should like to express my sincere thanks to Dr. Kamal K. Seth for suggesting the problem for this dissertation and my appreciation to him and Dr. H. W. Newson for their guidance and encouragement throughout the course of this investigation. I am particularly indebted to Dr. E. G. Bilpuch for his help and advice during the course of the experimental measurements reported here. I would also like to thank the entire personnel of the Nuclear Structure Laboratory for their assistance with the Van de Graaff generator. Mrs. Dorothy Brand Lehr was particularly helpful in analysis of data and I wish to acknowledge my indebtedness to her. I also wish to thank the staff of the Duke University Computing Laboratory for their helpful cooperation in the computational aspects of this investigation.

R.H.T.

CONTENTS

LIST OF FIGURES

LIST OF TABLES

OPTICAL MODEL PARAMETERS FROM AVERAGE TOTAL NEUTRON CROSS SECTIONS

CHAPTER I

INTRODUCTION

Lacking accurate knowledge of the detailed nature of nuclear forces, nuclear physics in the last fifteen years has mainly developed in the direction of phenomenonological models, each attempting to explain a particular class of phenomena. Amoungst the various models currently in vogue (see Chapter II), the nuclear Optical Model (Feshbach et. al., 1954) is perhaps the one with the largest number of successes to its credit. The model had its inception in certain observations in total neutron cross sections (Barschall, 1952). Though the model today is used to explain far more complex experimental observations (Jones, 1963), averaged neutron total cross sections still have the distinction of providing the most clear insight into some of the details of the model (Hodgson, 1963).

Average neutron total cross sections are usually considered as incoherent sums of cross section contributions due to various angular momenta. The contribution due to each angular momentum, in turn, is made up of two parts: the first is a slowly-varying part and is determined by the phase shift for potential scattering $\delta'(\ell)$, and the second is a part which shows relatively rapid variation with energy, and is determined by the so-called neutron strength function $S(\ell) = \langle \Gamma_n(\ell) \rangle / \langle D \rangle$. $\delta'(\ell)$ and $S(\ell)$ can be predicted by nuclear models, and their experimental determination provides a powerful way of testing the models.

The observation of the s-wave strength function maxima (Carter et. al.,

1954; Cote and Bollinger, 1955, 1958; Marshak and Newson, 1955, 1957) and the departure of $\delta'(\ell)$ from $\delta(\ell)$ for a hard sphere (Seth et. al., 1958) confirmed the correctness of the weak coupling theory of the nuclear optical model in contrast to the extreme compound nucleus model. After the initial measurements of s-wave strength functions, attempts were made to measure the p-wave strength functions. Early attempts in this direction met with qualitative success only (Boreli and Darden, 1958). Weston et. al. (1959) extracted p-wave strength function values from neutron capture cross sections in the kev region. They found indication of the splitting of the 2P neutron strength function peak, and intepreted it as being due to the spin-orbit part of the optical potential. Somewhat later, Gibbons et. al. (1961) measured capture cross sections with entirely different techniques and obtained results which were in qualitative agreement with those of Weston et. al. (1959) but which differed in two important respects. (1) The numerical value of strength functions derived by Gibbons et. al. (1961) were approximately a factor of three larger than those obtained by Weston et. al. (1959), and (2) from their data for a limited number of nuclei, Gibbons et. al. (1961) found no evidence of splitting due to a spin-orbit potential. In order to settle the differences which arose from these divergent results, Seth et. al. (1960) undertook the measurement of average neutron total cross sections in the kev region for nuclei in the region of the expected 2P and 3P strength function peaks. Their results bore out the essential correctness of the observations of Weston et. al. (1959). However, Seth et. al. (1963) did not measure or analyze cross sections for many elements removed from the p-wave strength function peaks. The purpose of the present dissertation is to fill the gaps left by the work of Seth et. al. (1963) and thus reinforce their con-

clusions about the p-wave strength functions. An important secondary reason for the present work is provided by the relative lack of information about $< \Gamma_n^{(o)} > / < D >$ and $\delta'(0)$ for the highly-deformed nuclei in the atomic weight region 140 - 240.

CHAPTER II

THEORY

In this chapter, we wish to present the theoretical background for the experiments reported in this dissertation. In Section B, we first give an introduction to the theory of resonance reactions as it applies to the theory of average total cross sections. In Section C, we discuss the nuclear Optical Model in relation to the simple potential-well model and the compound nucleus model and develop the connection between the parameters of the theory of average cross sections and those of the optical model.

A. NOTATION

In the following pages we shall use a notation that is largely derived from standard texts on theories of nuclear resonance reactions, e.g., Blatt and Weisskopf (1952), Lane and Thomas (1958), and Feshbach (1960). In the interest of simplicity many subscripts are often omitted whenever such omission is not likely to cause confusion.

1. a = Atomic weight of target nucleus. (1)
2. E = Energy of incident neutron of mass m.
3. $\lambda\!\!\!^{-} = k^{-1} = \lambda/(2\pi) = \{\hbar^2/(2me)\}^{1/2}\{a+1)/a\}^{1/2}$ = Dirac wave length of relative motion of neutron.
4. $\vec{I}, \vec{\ell}, \vec{J}$ = target spin, relative angular momentum, and total spin $(\vec{J} = \vec{I} + \vec{\ell} + \vec{1}/2)$ of a state, respectively
5. $g(J) = (1/2)\ (2J + 1)/(2I + 1)$ = Statistical weight factor for spin J.
6. $R = r_o a^{1/3}$ = nuclear radius.
7. $\rho = kR$
8. $\delta(\ell) = \tan^{-1}\left[-j_\ell(\rho)/n_\ell(\rho)\right]$ = hard sphere phase shift (where $j_\ell(\rho)$ and $n_\ell(\rho)$ are spherical Bessel and Neumann functions respectively).
9. $\delta'(\ell J)$ = potential (or shape elastic) scattering phase shift, model dependent.
10. $\Gamma(\ell J)$ = total (full) width (at half maximum) of a virtual state.
11. $\Gamma_n(\ell J)$ = neutron (full) width (at half maximum) of a virtual state.
12. $\Gamma_\gamma(\ell J)$ = total radiative width.
13. $E_o(\ell J)$ = level energy, measured from neutron binding energy.
14. $x(\ell J) = 2\left[E_o(\ell J) - E\right]/\Gamma(\ell J)$
15. $v(\ell) = \rho^{-2}\left[j_\ell^2(\rho) + n_\ell^2(\rho)\right]$ = Blatt and Weisskopf's (1952) penetration factor.
16. $P(\ell) = \rho v(\ell)$ = Lane and Thomas' penetration factor.

17. $\Gamma_n^{(\ell)}(J) = \Gamma_n(\ell J)/\left[v(\ell)(E(eV)/1(eV))^{1/2}\right]$ = commonly used (by experimentalists) neutron "reduced" width*.

18. $s(\ell J)$ = spacing of two adjacent levels of the same ℓ and J

19. $D_{obs}(\ell)$ = average observed spacing of levels for a given ℓ but including all J.

20. $D(\ell J) = D_{obs}(\ell)/g(J)$ = average observed spacing of levels for a given ℓ and J.

21. $D_o = D(\ell J)(2J + 1)/2$ = reduced spacing

22. $< >$ = symbol for the energy average of quantity inside.

23. $S(\ell J) = < \Gamma_n^{(\ell)}(J) >/< D(\ell J) >$ = neutron strength function for a given ℓ and J.

---

*Thomas (1955) and Blatt and Weisskopf (1952) define neutron reduced width as

$$\gamma_T^2(\ell J) = \gamma_{BW}(\ell J) = \Gamma_n(\ell J)/2P(\ell)$$

This "reduction" removes explicit energy and "nuclear size" dependences and has the energy dimensions of the unreduced width $\Gamma_n(\ell J)$.

We will refer to this reduced width $\gamma_T^2(\ell J)$ and its square root $\gamma_T(\ell J)$, the reduced width amplitude, without the subscript "T".

$$\gamma_W^2(\ell J) = \Gamma_n(\ell J)/2kv(\ell) = R\gamma_T^2,$$

which is the definition due to Wigner, on the other hand, does not remove the explicit R dependence and has units of energy x length, and is less popular for the same reason. The experimentalists definition given above is <u>not</u> width referred to 1eV as is sometimes stated (that would be $= \Gamma_n(\ell J) \cdot \left[v(\ell, 1eV)(1eV)^{1/2}\right] \cdot \left[v(\ell, E)(E(eV)^{1/2})\right]^{-1}$. Instead it is a Wigner type reduced width with the numerical factors in k neglected and dimensions artificially corrected by multiplication by $(1(eV))^{1/2}$. Since some earlier work (Darden, 1955) used the Wigner definition, we relate

$$\Gamma_n^{(\ell)}(J) = 4.4\ \gamma_W^2(eV \cdot fermi) x 10^{-4}.$$

24. $\mathcal{S}(\ell J) = \langle \pi\Gamma_n(\ell J) \rangle / \langle 2D \rangle$

25. θ_D = Debye temperature in degree Kelvin.

26. Δ = (Boltzmann's const.) $2(T_{eff}E_o/a)^{1/2}$

27. $t = \left[\Delta/\Gamma(\ell J)\right]^2$

28. $\sigma_t = \sum_{\ell} \sigma_t(\ell) = \sum_{\ell} \sum_{J} \sigma_t(\ell)$ = neutron total cross section summed over all ℓ and J.

29. $\sigma_o(\ell J) = 4\pi\lambda\!\!\!^{-2} g(J)\Gamma_n(\ell J)/\Gamma(\ell J)$

30. $\sigma_p(\ell J) = 4\pi\lambda\!\!\!^{-2} g(J) \sin^2\delta'(\ell J)$

31. $\sigma_r(\ell J) = \sigma_t(\ell J) - \sigma_p(\ell J)$

32. $T_{p,r}(\ell J) = \exp\left[-n\, \sigma_{p,r}(\ell J)\right]$

33. $T(\ell J) = T_p(\ell J)T_r(\ell J)$

34. $A(\ell J) = \int_o^\infty \{1 - T_r(\ell J)\}dE$

Explicit Expressions and Constants Used:

35. $r_o = 1.45$ fermi (fermi = fm = 10^{-13}cm)

36. $\lambda\!\!\!^{-} = k^{-1} = 4.552/\left[E(\text{MeV})\right]^{1/2}$

37. $4\pi\lambda\!\!\!^{-2} = 2.603/E(\text{MeV})$ barns

38. $\rho = 0.2197\left[E(\text{MeV})\right]^{1/2} R$ (fermis)

39. $\Delta = 0.01857\left[\theta_D E(\text{eV})/A\right]^{1/2}$eV

40. $\delta(0) = \rho$, $\delta(1) = \rho -$ arctan ρ, $\delta(2) = \rho -$ arctan$\left[3\rho/(3 - \rho^2)\right]$

41. $v(0) = 1$, $v(1) = \rho^2/(1 + \rho^2)$, $v(2) = \rho^4/(9 + 3\rho^2 + \rho^4)$.

B. Average Total Cross Sections from the Theory of Resonance Reactions

A number of different formulations of the theory of resonance reactions have been proposed from time to time (Wigner and Eisenbud, (1947)); Feshbach (1960); Humblet and Rosenfeld (1961). The differences between these different approaches are conceptual, mathematical, and formal, but the formalisms are physically equivalent. The choice of a particular formalism in a particular problem must depend on the convenience of its use and on the simplest, most direct interpretation of its parameters in terms of the physical model under test. For this reason we have chosen to use the recently proposed formalism of Feshbach (1960) which permits a natural identification of its parameters with the parameters of the complex potential model. We present below a brief review of the different formalisms in order to bring out the reasons for our choice.

As is usual in low energy nuclear physics, we decompose total cross section into its relative angular momentum components

$$\sigma_t = \sum_{\ell} \sum_{J} \sigma_t(\ell J). \tag{2}$$

In this section we shall talk about $\sigma_t(\ell J)$ only and will therefore omit explicit mention of ℓJ from all quantities, g, τ, δ, E_o, etc. According to the well known optical theorem

$$\sigma_t = 2\pi\lambda^2 g\ [\mathrm{Re}(\tau)] \tag{3}$$

where τ is the diagonal element of the transition matrix. [The elements of the commonly known collision matrix U are related to those of τ as $\tau = 1-U$.]

It is usual to break up τ into two parts, τ_p, which varies smoothly and the τ_r which fluctuates rapidly, i.e., shows resonance behavior

$$\tau = \tau_p + \tau_r \qquad (4)$$

Correspondingly,

$$\sigma_t = \sigma_p + \sigma_r \qquad (5)$$

At this stage we must point out the essential arbitrariness in the decomposition of τ and correspondingly σ_t. More than that we note that the interpretation of σ_p is different in different formalisms. It varies from hard-sphere scattering to hard-sphere plus contribution of far away resonances, to scattering from a real potential. In all cases it can be written in terms of the phase shift δ'

$$\tau_p = 2ie^{i\delta'} \sin \delta' \qquad (6)$$

and therefore

$$\sigma_p = 4\pi\lambda^2 g \sin^2\delta'. \qquad (7)$$

τ_r and therefore σ_r has different forms when levels are isolated, partly overlapping, or largely overlapping and averaged.

In the neighborhood of well-isolated single levels all formalisms yield the same form of τ_r, namely

$$\tau_r = -i \exp[2i\delta'] \Gamma_n/[E - E_o - (i\Gamma/2)] \qquad (8)$$
$$= [2\Gamma_n/\Gamma(1 + x^2)][\cos 2\delta' + x \sin 2\delta' + i(x \cos 2\delta' + \sin 2\delta')]$$

and therefore we obtain the single level Breit Wigner formula

$$\sigma_r = \sigma_o[1 + x^2]^{-1}[\cos 2\delta' + x \sin 2\delta'] \qquad (9)$$

where

$$x = 2(E - E_o)/\Gamma.$$

The energy average of $Re(\tau_r)$ above can be simply obtained to

$$< Re(\tau_r) > = \frac{\pi < \Gamma_n > \cos 2\delta'}{< D >}$$

and therefore

$$< \sigma_r > = 2\pi^2 \lambda^2 g \frac{< \Gamma_n >}{< D >} \cos 2\delta'$$

or (10)

$$< \sigma_t > = 4\pi \lambda^2 g \, [\sin^2 \delta' + \beta \cos 2\delta']$$

where $\beta = \pi < \Gamma_n > / < 2D >$.

It should be pointed out that in order to preserve the unitary nature of the collision matrix we must require that β be less than or equal to 1 or $< \Gamma_n > / < D >$ be less than or equal to $(2/\pi)$.

For partially overlapping levels, the R-matrix theory gives extremely complicated results for the many channel case and no simple explicit expression can be written down. In the single channel case (elastic scattering only, $\Gamma = \Gamma_n$)

$$\sigma_r = \sigma_o [1 + x'^2]^{-1} [\cos 2\delta' + x' \sin 2\delta'] \qquad (11)$$

where

$$x' = [1 + \sum_m (2\Delta'_m / \Gamma_m x_m)] [\sum_m x_m^{-1}]^{-1} \qquad (12)$$

which reduces to

$$x' = [\sum_m x_m^{-1}]^{-1} \qquad (13)$$

when all level shifts $\Delta_m' = 0$. (This is rigorously possible only for $\ell = 0$ resonances).

For the many-level, many-channel case Feshbach's formalism yields the particularly simple result

$$\sigma_r = 2\pi\lambda^2 g \, \mathrm{Re}\{-ie^{2i\delta'} \sum_m [B_m/(E - W_m)]\} \qquad (14)$$

where B_m and W_m are in general complex and not simply related to the widths Γ_{nm} and complex level energies $(E_{om} - i\Gamma_m)$. Thus all the complicated aspects of level-level interference, etc. are contained in the lack of a precise relation between B_m and W_m.

When many levels overlap or the energy average over a large number of levels is considered, obviously the individual widths and level energies cannot decide the overall behavior of $< \sigma_t >$. They might determine local fluctuations in the over-all behavior, but the main course of $< \sigma_t >$ should rather depend on statistical properties of widths and spacings and on the specific nature of correlations between the signs of the reduced width amplitudes. Further, the different expressions $< \sigma_t >$ will also reflect the different conventions in the decomposition of $< \sigma_t >$ into the slowly varying energy part and the resonance part.

a) Using the R-matrix theory and assuming that the signs of γ_m are completely correlated (Newton, 1952), and that all levels have a uniform width $< \Gamma >$ and all spacings are $= < D >$, Teichmann (1950) obtained

$$< \sigma_t > = 4\pi\lambda^2 g \, [\sin^2\delta' + \mathcal{S} \, (1 + \mathcal{S})^{-1} \cos 2\delta'] \qquad (15)$$

It is worthwhile pointing out that redefining $\mathcal{S}' = \mathcal{S}/(1 + \mathcal{S})$ leads to the single level expression Eq. (10). Of course for $\mathcal{S} \ll 1$, $\mathcal{S}' \approx \mathcal{S}$.

b) In the last few years, following the pioneering work of Porter and Thomas (1956) and Wigner (1956) it has been shown that the probability distributions of widths and spacings are

$$P(\Gamma_n)d\Gamma_n = (2\pi x)^{-1/2} \exp(-x/2)dx, \quad x = \Gamma_n/\langle \Gamma_n \rangle \qquad (16)$$

$$P(s)ds = \frac{\pi}{2} y\, e^{-\pi y^2/4}dy \qquad y = s/\langle s \rangle \equiv s/\langle D \rangle \qquad (17)$$

Further, work by Blumberg and Porter (1958) has shown that these distributions follow from the assumption that the matrix elements of the compound nucleus Hamiltonian whose eigenvalues are the energy levels and whose eigenvectors are the wave functions (which determine the widths) are random and have Gaussian distributions. The randomness assumption has been used by Thomas (1955) to derive expressions for average cross sections.

For $\langle \Gamma \rangle >> \langle D \rangle$

$$\langle \sigma_t \rangle = 4\pi\lambda^2 g \left\{ \frac{[\sin\delta' - PR^\infty \cos\delta]^2 + \phi\,[1 + \phi \cos^2\delta]}{[1+\phi]^2 + [PR^\infty]^2} \right. \qquad (18)$$

where R^∞ is the Stieltje's transform of $\phi/\pi\rho$

For $\langle \Gamma \rangle / \langle D \rangle$ the result cannot be simply written. (Lane & Thomas, 1958). Presumably it is much like the average of the single level formule with the potential phase shift and the penetrabilities modified by contributions from far away levels.

Eq. (18) presents the typical problem in the use of the R-matrix theory for average cross sections. It cannot be simply decomposed into two parts, one of which can be identified with potential scattering and the other with $\langle \sigma_r \rangle$. Following Seth (1959b) if we expand Eq. (18) in powers of ϕ, we get

$$\langle \sigma_t \rangle = 4\pi\lambda^2 g \{\sin^2\delta' + \phi \cos 2\delta' - \phi^2 \cos 2\delta' + \ldots\} \qquad (19)$$

where

$$\delta' = \delta - \tan^{-1} PR^{\infty} \qquad (20)$$

In this expression the term in ϕ^2 has approximately the same energy dependence as potential scattering and potential scattering can be redefined to include it. Even then the above expression is not accurate since $\phi \gg 1$ and higher powers should not be neglected without careful consideration (Seth 1959(b)). Thus in nearly all cases of interest when ϕ is large Eq. (18) itself must be used.

As mentioned before, this presents problems in identifying the parameters of (18) with those of the optical model whose phase shifts lend themselves directly to an expression of the type of Eq. (10).

c) For completely overlapping levels or cross-sections averaged over a large number of levels, Feshbach's formalism once again yields a relatively simple form once the randomness hypothesis is used. One obtains

$$\tau_r = -ie^{2i\delta} \sum_m \frac{\Gamma_{nm}}{(E - E_{om}) + (i/2)(\Gamma_m + \Gamma_m')} \qquad (21)$$

where the only quantity distinguishing the above from a sum of single level terms of the type of Eq. (8) is Γ_m' which has an average value zero. In other words Eq. (21) states that, in this situation, the sum of single level formulae does not provide a true description everywhere, but it does on the average. This result is independent of the number of open channels and on whether $< \Gamma > / < D >$ is much less than, or greater than unity. This is an extremely satisfying result which lends itself easily to energy averaging. It yields

$$< \tau > = < \tau_r > + < \tau_p > = 1 - \exp(2i\delta')[1 - 2\phi] \qquad (22)$$

or

$$\langle \sigma_t \rangle = 4\pi\lambda^2 g[\sin^2\delta' + \pi/2\cos 2\delta'] \tag{23}$$

which is the same as Eq. (10), the cross section obtained by averaging the single level formula. Notice that no terms quadratic or higher in δ occur here. The phase shift δ' here will be complex if either channel spin or ℓ is changed in the interaction or if non-resonant inelastic scattering ("direct interaction") is present. In general

$$\delta = \alpha + i\beta \tag{24}$$

In the complex potential model of the nucleus one obtains complex phase shifts $\xi + i\eta$ in terms of which

$$\bar{\tau} = 1 - \exp[2i(\xi + i\eta)] \tag{25}$$

If we equate

$$\langle \tau \rangle = \bar{\tau}$$

$$\exp[2i\xi - 2\eta] = \exp[2i\alpha - 2\beta](1 - 2\delta)]$$

Therefore if $2\delta < 1$

$$\xi = \alpha$$

$$e^{-2\eta} = e^{-2\beta}(1 - 2\delta) \tag{26}$$

and if $2\delta > 1$

$$\xi = \alpha + \pi/2$$

$$e^{-2\eta} = e^{-2\beta}(2\delta - 1)$$

These relations provide a very direct way of obtaining δ and δ from the calculated complex phase shifts $(\xi + i\eta)$ of the optical model. It has been shown by Feshbach that if we define α and δ via the low energy limits then one obtains an expression quadratic in δ as in Eq. (19). Thus the quadratic term in Eq. (19) must be regarded as essentially avoidable.

C. The Nuclear Optical Model

In this section we describe the nuclear optical model. We develop our considerations of this model somewhat historically in order to bring out its nature which is intermediate between the nuclear shell model and the extreme compound nucleus model.

The potential-well model, and independent-particle model, was first proposed by Bethe (1937). In this model, the nucleus is thought of as a system of independent particles, each moving in the potential created by the others. This type of potential well model is successful in explaining phenomena such as the low-lying states of a nucleus, ground state magnetic and electric moments, and the like. The potential is real, and in the simplest description, may be considered to have the rectangular shape

$$\begin{aligned} V(r) &= -V_o \qquad r < R \\ V(r) &= 0 \qquad\quad r > R \end{aligned} \tag{27}$$

where R is defined as the nuclear radius

$$R = r_o A^{1/3} = 1.45 \times 10^{-13} A^{1/3} \text{cm}$$

The rectangular potential well may also be used to describe the interaction of an incident nucleon with a target nucleus. For the case of incident neutrons, the value of V_o has been found to be about 42 MeV. In the real potential well, one can only have potential (shape-elastic) scattering or radiative capture. Since the transit time of the neutron through the well is only about 10^{-21} sec., the probability of radiative transition to a bound state of the system is negligibly small. One may solve the wave equation to deter-

mine the single-particle energy levels; the levels occur wherever

$$KR = n\pi,\ n = 1, 2, \ldots \quad \ell \text{odd}$$
$$KR = (n + 1/2)\pi,\ n = 0, 1, 2, \ldots \quad \ell \text{even} \qquad (28)$$

provided the neutron energy $E_n \ll V_o$. The 3S and 4S states occur at zero energy for a = 58 and 160, while the 2P, 3P, and 4P states are predicted at approximately a = 30, 101, and 239. For a given a, the spacing of these states is of the order of several MeV.

In order to account for ground state properties, a spin-orbit interaction term was introduced into the independent particle shell model (Jensen and Mayer, 1949). This term splits each $\ell > 0$ state into two. The p-wave states are thus split into $P_{3/2}$ and $P_{1/2}$ states. The $P_{3/2}$ state occurs at lower energy for a given nucleus and at lower A for a given energy than the $P_{1/2}$ state. The separation between the two states is determined by the magnitude of the spin-orbit interaction.

This real potential well model fails for several reasons. First, potential scattering, and radiative capture are not the only interactions between an incoming nucleon and a nucleus. Also the magnitude of radiative capture predicted by this model is very small, whereas actually at low neutron energies radiative capture predominates over other interactions. Besides this, heavy nuclei generally have resonance spacings of the order of 10eV, rather than of several MeV as predicted by this model.

In order to account for the observed phenomena, Bohr (1936) introduced the compound nucleus model, a type of strong-interaction model. Since the nuclear interaction is very strong, one would expect a nucleon incident upon a nucleus to interact strongly with the nucleus, sharing its energy rapidly

with the target nucleons. Bohr (1936) proposed that an incident particle interacts immediately with the nucleus forming a compound state in which all nucleons share the total excitation energy. This compound state lasts about 10^6 times longer than the 10^{-21} sec. transit time for the incident nucleon to move a distance of about one nuclear diameter. Taking into account the conservation laws the compound state should then decay in a mode entirely independent of the formation. The energy widths predicted from this model $\Gamma = \hbar/10^{-15}$ sec are found to be of the order of an eV, in agreement with the widths observed for heavy nuclei. Also since many nucleons share the excitation energy, the quantized virtual energy states will be closely spaced, in agreement with the observed spacings.

In the compound-nucleus model, there can be modes of decay besides shape-elastic scattering and radiative capture; viz, reaction or fission. The probability of decay of a given state is proportional to the energy width of the compound state Γ. The branching ratio that this state will decay, through any given mode x, is Γ_x/Γ where $\Gamma = \sum_x \Gamma_x$. Γ_x is a partial width, and Γ is the total width of a compound state.

The model predicts (in agreement with experiments) that the lifetime of the compound state is relatively long, and the radiation width Γ is large, since radiative transitions to bound nuclear states have a much higher probability of occuring than for the real potential well model.

In this model, in addition to the hard sphere elastic scattering compound nucleus formation and decay contribute to cross sections. The hard sphere scattering results from the low penetrability of the nucleus to neutrons having non-resonant energies, and is analogous to the potential scatter-

ing of the real potential model. The average compound nucleus cross section may be calculated (Feshbach et al., 1947) by considering transmission across the nuclear boundary.

$$\bar{\sigma}_t = \sigma_p + \bar{\sigma}_c, \tag{29}$$

where $\bar{\sigma}_c$ = geometric cross section, $\pi(R + \lambda\!\!\!^{-})^2$ times transmission, T, of the nuclear surface, i.e.,

$$\bar{\sigma}_c = \pi(R + \lambda\!\!\!^{-})^2[4kK/(k + K)^2]. \tag{30}$$

If the compound nucleus has a uniform level spacing $< D >$, the period of motion in which the nucleus returns to its original configuration, P, is (Blatt and Weisskopf, 1952)

$$P = 2\pi\hbar/ < D >.$$

Since the lifetime, τ, of the state

$$< \tau > = \hbar/ < \Gamma_n > = P/T$$

$$< \Gamma_n > = \hbar/< \tau > = (< T >/2\pi)< D >$$

or

$$< \Gamma_n >/< D > = < T >/(2\pi).$$

or

$$< \Gamma_n^o >/< D > = < \Gamma_n/\sqrt{E} >/< D > = \frac{2}{\pi}\frac{k}{K}\frac{1}{\sqrt{E}} \tag{31}$$

According to equations (29) and (30), $\bar{\sigma}_t$ for all nuclei is a monotonically decreasing function of energy, and the strength function, $< \Gamma_n^o >/< D >$, is independent of atomic weight. For a 42 MeV deep potential

$$< \Gamma_n^{(o)} >/< D > = 10^{-4}$$

In contradiction to the above predictions Barschall(1952) showed that the average total cross section, for neutrons in the higher kev and in the MeV range exhibited broad resonance behavior, both as a function of A and E_n. Carter et al. (1954), made the first determinations of the s-wave strength function $< \Gamma_n^{(o)} > / < D >$ for $E_n \approx$ a few eV and found that it has a resonant behavior as a function of atomic weight.

The evident failures of both the real potential well model and the compound nucleus model led to the optical model.

The optical model represents the nucleus as a complex potential well. The real part of the potential is similar to the shell model potential well. A small imaginary term added to the real potential accounts for reactions and compound nucleus formation. The complex potential predicts both scattering and absorbtion of incoming nucleons, in analogy to the scattering and absorption of light rays by a medium having a complex refractive index.

In 1949, Fernbach, Serber, and Taylor (1949) analyzed neutron scattering near 100 MeV in terms of a nuclear potential having a complex refractive index. Feshbach, Porter, and Weisskopf (1954) extended the idea of using a complex potential to low energy neutron interactions. In this model as contrasted to the compound-nucleus model, the incident particle does not necessarily interact with other nucleons, but has a mean free path of several nuclear diameters in the nuclear matter. Potential scattering occurs if there is no such interaction, otherwise a compound state is formed; the probability of this absorption being dependent upon the magnitude of the imaginary term.

Feshbach et.al. (1954) defined the various cross sections as

$$\sigma_t = \sigma_{reaction} + \sigma_{elastic}$$

$$\sigma_{elastic} = \sigma_{compound\ elastic} + \sigma_{shape\ elastic} \qquad (32)$$

$$\sigma_{compound\ nucleus\ formation} = \sigma_{reaction} + \sigma_{compound\ elastic}$$

As a potential, they used the rectangular-well potential

$$V(r) = -V_o(1 + i\zeta) \qquad r \leqslant R$$

$$= 0 \qquad r > R \qquad (33)$$

where again $R = 1.45 \times 10^{-13}\ a^{1/3}$ cm, the nuclear radius. The predictions of this model which are of direct interest to us are related to neutron average total cross sections. According to this model $\langle \sigma_t \rangle$ is not a monotonic function of either energy or atomic weight as the Feshbach - Peaslee - Weisskopf model (Eq. 30) predicts. Instead $\langle \sigma_t \rangle$ should exhibit single particle resonances as a function of energy, as noticed in the work of Barschall et al. (1952), and as a function of atomic weight, as brought out in the lower energy work of Marshak and Newson (1955), Cote´ et al. (1955), Hughes et al. (1958), and Seth et al. (1958).

Feshbach et al. (1954) suggested two important modifications to the square-well model they had proposed. The first requires taking into account the well-known aspherical nature of a large number of nuclei, particularly those with atomic weight greater than 130. This was done by Chase, Wilets, and Edmonds (1958) and their calculations succeeded in reproducing the irregular splitting of the peak in $S(0)$ near $a \approx 140$ observed by Hughes et al. (1958), and the splitting of the $\delta'(0)/\delta(0)$ peak near $a \approx 160$, observed by Seth et al. (1958). In this dissertation we present more detailed and accurate

results for $S(0)$ and $\delta'(0)/\delta(0)$ for nuclei with $A > 130$ and compare them with the more recent theoretical calculations of Perey and Buck (1962).

The second modification suggested by Feshbach et al. (1954), was the inclusion of a spin-orbit potential in the complex potential model to account for the observed polarization effects. Weston, Seth, Bilpuch and Newson (1960) pointed out that a spin-orbit potential would also split each strength function resonance for $\ell > 1$ into two. They compared their determinations of p-wave strength functions, $S(1)$, from average capture cross sections with the predictions of a square-well complex potential model with a spin-orbit potential added to it.

$$V = V_o(1 + i\xi) + V_{so}\vec{\ell}\cdot\vec{s} \qquad (34)$$

$$= V_o\left[1 + i\xi + (\beta/2)\{-1 \pm (2\ell + 1)\}\right], \quad r \leq R$$

$$= 0 \qquad , \quad r > R.$$

As mentioned in the introduction, their experimental results and their square-well analysis lead them to believe that the 3P resonance was split. In this dissertation we attempt to present $S(1)$ results obtained by the analysis of our measured $\langle \sigma_t \rangle$ and compare them to the more sophisticated predictions now available from the work of Perey and Buck (1962).

CHAPTER III

EXPERIMENTAL

A. Measurement of Cross Section

The cross section measurements reported in this dissertation were made using the Duke University 4 MeV Van de Graaff generator. The floor plan of the experimental setup is shown in Fig. 1. A monoenergetic proton beam from the Van de Graaff generator was deflected by a 60° steering magnet. The H^+ beam was bent 60°, while the HH^+ beam (which constitutes a small fraction of the output of the RF ion source) was simultaneously bent through 44°25'. The HH^+ beam was focused on the object slits of a 90° cylindrical electrostatic analyzer and the error signal derived from these object slits was used to control the corona stabilizer of the Van de Graaff. The HH^+ beam passed through the electrostatic analyzer, then through a pair of image slits to a beam catcher. The 60 and 400 cycle beam energy variations were corrected by the use of a device called the "homogenizer" (Parks, Newson, and Williamson, 1958).

The H^+ beam (whose energy is accurately determined) was incident on a Li target evaporated in vacuum on a thin (5 to 10 mils) Ta backing. The cylindrical analyzer was calibrated with respect to the Li(p,n) forward threshold energy which was assumed to be 1.8811 MeV at 0° (Gibbons and Newson, 1960).

Neutrons produced by the $Li^7(p,n)$ Be^7 reaction were accepted between the cone angles of 18° and 20°. The conical opening was divided into two separate parts, each of which was separately viewed by independent banks

Figure 1. Floor Plan for the Duke University 4 MeV Van de Graaff.

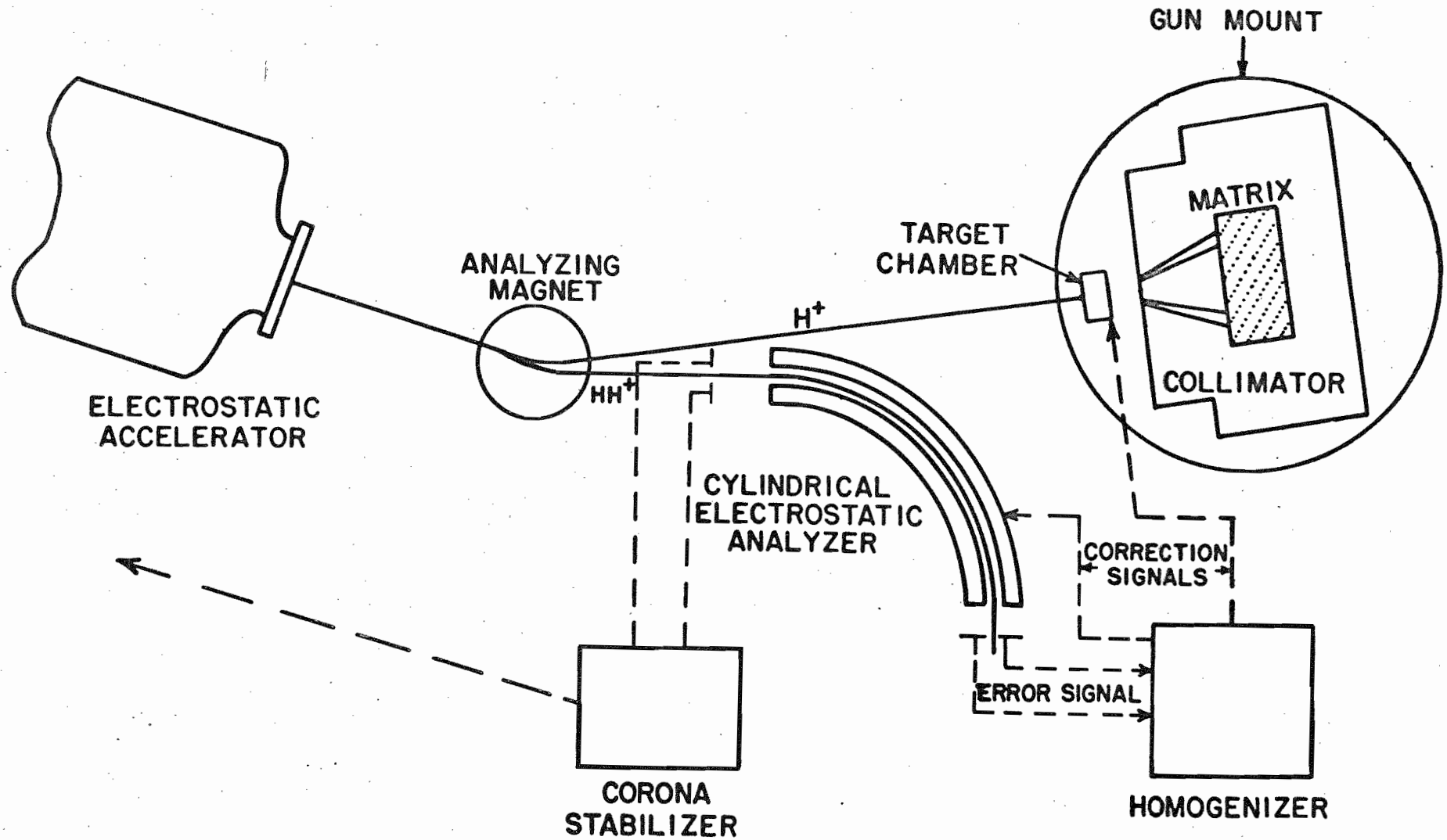
GUN MOUNT
MATRIX
COLLIMATOR
TARGET CHAMBER
ANALYZING MAGNET
H^+
HH^+
ELECTROSTATIC ACCELERATOR
CYLINDRICAL ELECTROSTATIC ANALYZER
CORRECTION SIGNALS
ERROR SIGNAL
CORONA STABILIZER
HOMOGENIZER

of BF_3 counters embedded in separate polyethylene moderating matrices. The collimator assembly and the Li target chamber have both been described in detail elsewhere (Nichols, Bilpuch, and Newson, 1959). The only difference between the present arrangement and the one described by Nichols et al. (1959) is that the collimator tank is now mounted on a gun mount and has been rotated through 180° to use the neutrons at 18° to 20° angles rather than those at 160° to 162°. The new arrangement has been described by Bowman et al. (1962). The basic measurement consisted of counting the number of neutrons in one bank of counters relative to the counts in the other bank. Alternately, one of the two banks was shielded by the sample while the other was open.

B. Neutron Energy Considerations

1. At 19° the Li(p,n) reaction gives two monoenergetic groups of neutrons between the 19° threshold (at E_p = 1.8853 MeV) and the 90° threshold at E_p = 1.923 MeV. These are illustrated in Fig. 2. As can be seen, at the 19° threshold the two groups have the same energy, namely 27.5 kev; as the proton energy is increased, the two groups begin to differ in energy substantially. Fortunately, the yield of the lower energy group falls off rapidly. Thus, for example, at proton energy of 1.910 MeV, the lower energy group has an energy of 1 kev, and a yield of 0.5%, while the higher energy group has an energy of 94 kev and a yield of 99.5%. Thus, while in theory at the 19° ±1° acceptance angle monoenergetic neutrons are only available above an energy E_n = 116 kev (E_p = 1.923 MeV), in practice, the rapidly decreasing yield of the low energy group makes it possible to regard neutrons of energy above approximately 100 kev as essentially monochromatic. The following calculation illustrates the point. Let $\sigma_t'(E_U)$ represent the measured cross section at the upper group energy E_U, and $\sigma_t(E_U)$ the true cross

Figure 2. Energies and Intensities of the Two Neutron Groups from the $Li^7(p,n)Be^7$ Reaction in the Neighborhood of the 19° Threshold.

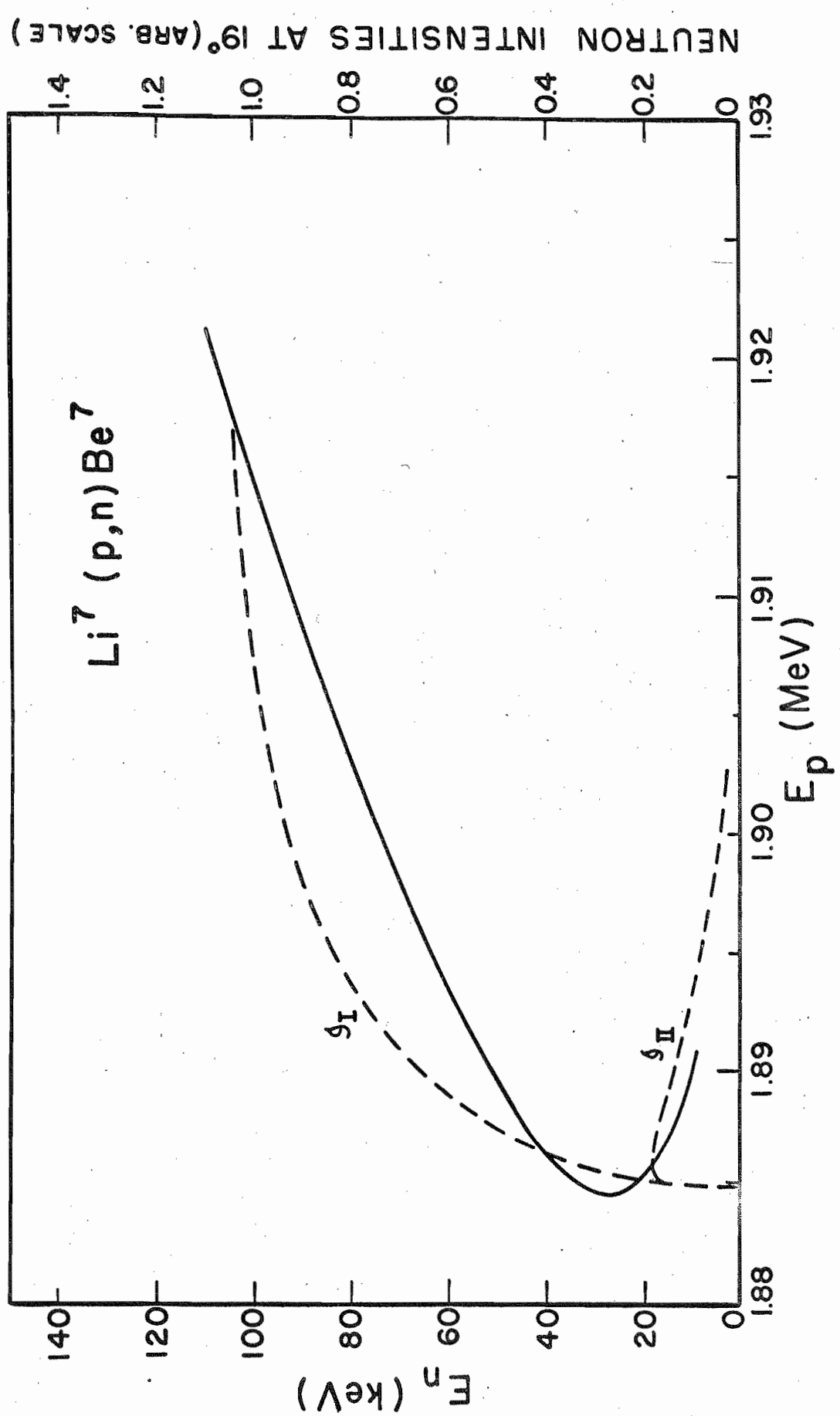
NEUTRON INTENSITIES AT 19° (ARB. SCALE)
1.4
1.2
1.0
0.8
0.6
0.4
0.2
0
1.93
1.92
1.91
1.90
1.89
1.88
E_p (MeV)
E_n (keV)
140
120
100
80
60
40
20
0
$Li^7(p,n)Be^7$
g_I
g_{II}

section at energy E_U. Let $\sigma_t(E_L)$ be the true cross section at the lower group energy E_L. Let 'f' be the fraction of the lower energy component. In order that the measured cross section $\sigma_t'(E_U)$ be in error by less than 2%, we require that

$$\{\sigma_t'(E_U)/\sigma_t(E_U)\} - 1 \quad < 0.02 \tag{35}$$

Since

$$\sigma_t'(E_U) = f\sigma_t(E_L) + (1 - f)\sigma_t(E_U) \tag{36}$$

we must have

$$f \left| \{\sigma_t(E_L)/\sigma_t(E_U)\} - 1 \right| \quad < 0.02 \tag{37}$$

Even in the worst case, namely E_L = 1 kev, E_U = 94 kev, the ratio $\sigma_t(E_L)/\sigma_t(E_U)$ is not greater than 5. Thus

$$f < 0.005 \qquad \text{or } 0.5\% \tag{38}$$

i.e., up to 0.5% contamination of the low energy group is tolerable. In most cases, the ratio $\sigma_t(E_L)/\sigma_t(E_U)$ is much less than 5, and hence the measured cross sections at values of E_U even less than 80 kev have an error much less than 2%. Whenever the correction was larger than 2%, it was applied to the measured cross sections using the results of our strength function analysis to obtain $\sigma_t(E_L)/\sigma_t(E_U)$. For a large number of nuclei, this ratio is found to be close to unity, in which case no correction is required. For a detailed discussion of this point, see Appendix 1.

2. Be^7 has an excited state at 430 kev. Thus, at 19°, monoenergetic neutrons may be obtained from the $Li(p,n)Be^7$ up to E_n = 620 kev. However, the yield of the second group is considerably less than 1% (Bevington, Rolland, and Lewis, 1961) below E_n = 650 kev. At E_n = 650 kev, the energy of these neutrons is E_n = 100 kev. The cross section for most elements does not change

greatly between E_n = 100 kev and E_n = 650 kev. For the worst case we find

$$\sigma_t(100)/\sigma_t(650) = 1.7 \qquad (39)$$

The error due to the cross section contribution of the lower energy neutrons will therefore always be less than 0.7% of the observed value.

The measurements reported here were made between E_n = 27.5 kev and E_n = 650 kev, with energy steps ΔE_n = 10 kev between 30 and 60 kev, ΔE_n = 20 kev between 60 and 180 kev, ΔE_n = 10 kev between 180 and 200 kev, and ΔE_n = 5 kev for higher energies.

C. Resolution

For most of the nuclei investigated, the mean spacing of the compound nuclear levels is of the order of 1 to 100 eV. Thus for the average cross section measurements, a resolution of 10 to 15 kev is sufficient. Among the sources which contribute to the effective neutron energy spread, the proton energy spread and the Doppler motion of the nuclei conbribute much less than 1 kev. The 2° cone opening corresponds to an energy spread from about 2.6 kev (at 100) to 5 kev (at 650 kev). A Li target which corresponded to a neutron energy spread of approximately 10 kev was therefore used; the final neutron energy spread was between 10 and 15 kev. This dictated the choices of energy steps in data taking, as described in Section B.

D. Background and Scattering Corrections

The usual counting rates during these experiments were between 30,000 and 200,000 counts per minute. The background in this experiment arises mainly from two sources: (1) the usual electronic and cosmic ray backgrounds, these combined were always less than 0.1% of the usual counting rates, and (2) the background due to the scattered neutrons in the room.

These neutrons presumably reach and get counted in the detector matrices from directions other than the cone opening. Their number can be determined by counting with completely closed cones. For neutron energies between 50 and 650 kev, this background was found to be essentially constant and equal to about 80 counts per minute, i.e., $\ll 0.2\%$ of the open beam count rate. Since this measurement includes the background of the first kind, it is concluded that the overall background was less than 0.2%.

There are two other main sources of background neutrons. Neutrons emitted at angles other than 19° ± 1° may be scattered by the Ta backing into the collimator (extaneous neutrons). Further, neutrons emitted at angles other than 19° ± 1° may be scattered into the collimator by the sample itself (inscattering). The first of these effects could not be measured in our experiments; however, a good estimate of its magnitude for the 160° arrangement is available from the work of Nichols et al. (1959) and similar information for the 20° arrangement is given by Bowman, Bilpuch, and Newson (1962). For the Ta backings used (5 mils or 10 mils), this background for the 20° case is between 2 and 3% of the counting rate. No measurements of the inscattering effect were made. An estimate of single-scattering inscattering was made using a formula similar to that quoted by Miller (1960). The indicated effect was $\sim 0.1\%$ reflecting the goodness of our geometry. While double-scattering and higher order multiple scattering could not be easily calculated, it is expected that contributions due to these will be smaller still. For this reason no corrections for inscattering were applied to the data. The subject is, however, presently under experimental investigation.

E. Samples

In Table 1, we summarize the pertinent information about the various samples used in this experiment. As may be noticed from the table, In, Sb, and I were used as samples with 2" x 4" area. The In sample was in the form of rectangular plates, while Sb and I were pressed in boxes with 15 mil Ta and 1/32" teflon faces, respectively.

La, Hf, Ta, Ir, Th, U were used as solid metal slabs 1/2" x 1" in area. Ru, W, Re, Os samples were made by pressing 350 mesh powders into the shape of rectangular parallelopipeds 1/2" by 1" in area, and canned in a box made of 3 mil silver foil. The Hg container was made out of thin welded stainless steel. Appropriate compensators were used (for measuring the open beam counts) for all canned samples.

According to the suppliers the samples were better than 99% chemically pure, and care was taken during pressing and canning to prevent oxidation and absorption of water vapor.

The sample thicknesses were determined by measuring the cross sectional area and weighing the samples. Measurements were reproduceable to within 0.2%. However, angular sample positioning errors as large as 1% are considered possible. The estimated error in effective sample thicknesses n was therefore taken as ±1%.

F. Transmission Measurements

The 2" x 4" samples of In, Sb and I were used close to the face of the collimator, while the 1/2" x 1" samples were used close to the Li target (Bowman et al., 1962). A single sample was mounted such that it could alternately shadow one detector bank completely and at the same time allow the other detector bank to see the unattenuated flux from the Li target. At the

Table 1

Data on Samples

Element	Isotopic Abundance[1] % (I)		t used	Effective Sample Thicknesses n in (atoms/barns)
Ru [2]	70·2	(0)	256	0.0412, 0.107, 0.148
	29·8	(5/2)	1024,2048	
In [3,4]	100.0	(9/2)	2048	0.0387, 0.0505, 0.0892
Sb [2,4]	100.0	(5/2),(7/2)	256,512	0.0332, 0.113, 0.146
I [2,4]	100.0	(5/2)	256,512	0.0323, 0.0640, 0.0861
La [3]	99·9	(7/2)	32,128	0.0169, 0.0324
Hf [3]	67·8	(0)	16	0.0238, 0.0606, 0.0804
	32·2	(7/2,9/2)	128,256	
Ta [3]	100.0	(7/2)	64,128	0.0356, 0.0889, 0.142
W [2]	85·6	(0)	2	0.0414, 0.0892, 0.130
	14·4	(1/2)	4,16	
Re [2]	100.0	(5/2)	128,256	0.0349, 0.0594, 0.0942
Os [2]	82·3	(0)	8	0.0384, 0.0574, 0.0952
	17·7	(1/2,3/2)	8,32	
Ir [3]	100.0	(3/2)	64,256	0.0222, 0.0440, 0.0770
Hg [5]	69.9	(0)	1/4	0.0229, 0.0604, 0.103
	30·1	(1/2,3/2)	2,4	
Th [3]	100.0	(0)	128	0.0294, 0.0604, 0.103
U [3]	100.0	(0)	128	0.0251, 0.0476, 0.0927

1. Abundances above are given for sums of even-A (I=0) and odd-A (I≠0) isotopes.
2. Pressed powder.
3. Metallic slab.
4. Cross sectional area 2" x 4". All others are 1/2" x 1" in area.
5. Canned liquid.

end of half the measurement, the sample "in" and "out" positions were interchanged. On each side, 50,000 out counts were counted. If I, O, and B denote the sample in, sample out, and background counts, respectively, and subscripts L and R denote the positions left and right,

$$< T > = (< T_L > < T_R >)^{1/2} \tag{40}$$

where

$$T_{L,R} = (I_{L,R}-B)/(O_{L,R}-B). \tag{41}$$

There are a number of advantages in this method of determining the transmission. At any instant, both in and out counts are taken; thus beam intensity fluctuations are automatically corrected for, without requiring an additional monitor. Further, since the position of in and out are interchanged, any long-term (slower than a minute) fluctuations are reflected in the difference between T_L and T_R, and are removed, to the first order, from T. For the same reason, the difference in the efficiencies of the two detector banks and their separate electronics is also eliminated.

The average total cross section $\bar{\sigma}_t$ is obtained from the transmission as

$$\bar{\sigma}_t = -(1/n) \log_e < T >.$$

The cross sections measured are displayed in Fig. 3.

G. Errors

The error in the cross section measurement can be calculated as follows. Since

$$\Delta f(x, y, z \ldots) = \left[\left(\frac{\partial f}{\partial x} \Delta x\right)^2 + \left(\frac{\partial f}{\partial y} \Delta y\right)^2 + \left(\frac{\partial f}{\partial z} \Delta z\right)^2 + \ldots \right]^{1/2} \tag{42}$$

then

Figure 3. Measured Neutron Total Cross Sections. The thick sample cross sections, which differ from these only below E_n = 100 kev, are not shown.

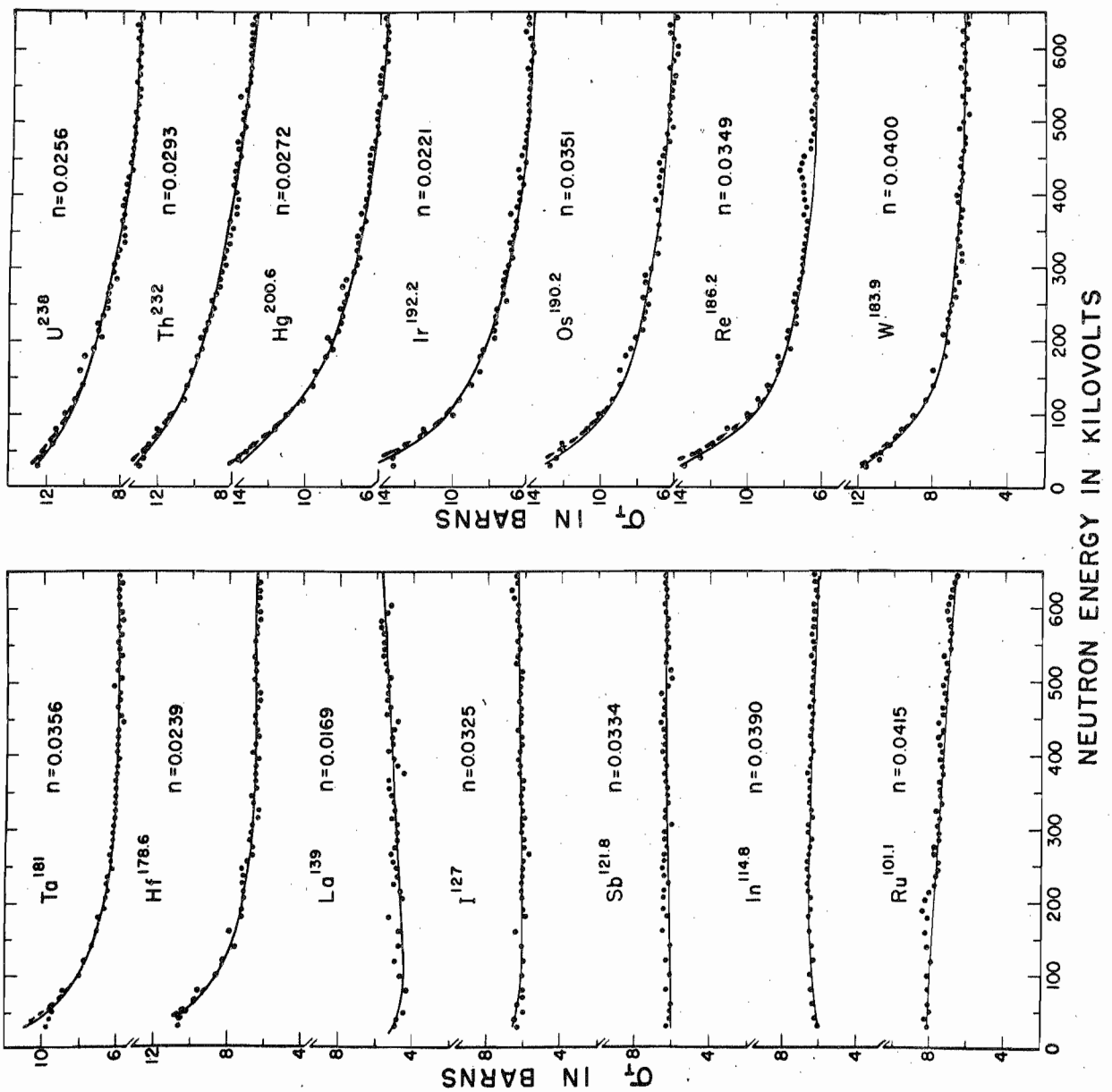
U^{238} n=0.0256
Th^{232} n=0.0293
$Hg^{200.6}$ n=0.0272
$Ir^{192.2}$ n=0.0221
$Os^{190.2}$ n=0.0351
$Re^{186.2}$ n=0.0349
$W^{183.9}$ n=0.0400
Ta^{181} n=0.0356
$Hf^{178.6}$ n=0.0239
La^{139} n=0.0169
I^{127} n=0.0325
$Sb^{121.8}$ n=0.0334
$In^{114.8}$ n=0.0390
$Ru^{101.1}$ n=0.0415
σ_t IN BARNS
NEUTRON ENERGY IN KILOVOLTS

$$\Delta\sigma_t = \sigma_t\left[\left(\frac{\Delta n}{n}\right)^2 + \left(\frac{\Delta T}{T \log_e T}\right)^2\right]^{1/2} \tag{43}$$

where

$$\Delta T = (T/2)\left[\sum_i (N_i - B)^{-1}\right]^{1/2} \tag{44}$$

where N_i is successively I_L, I_R, O_L, and O_R.

This error was calculated upon specification of $\Delta n/n$ in a computer program (called PROD, Program for Reduction of Data). A typical input and output of the program is given in Appendix IV.

CHAPTER IV

ANALYSIS

The average total cross section is given by

$$\langle \sigma_t \rangle = \sum_{\ell} [\sigma_p(\ell) + \langle \sigma_r(\ell) \rangle] \tag{45}$$

where

$$\sigma_p(\ell) = 4\pi\lambda\!\!\!^{-2}(2\ell + 1)\sin^2\delta'(\ell)$$

$$\langle \sigma_r(\ell) \rangle = 2\pi^2\lambda\!\!\!^{-2}(2\ell + 1)S(\ell)v(\ell)\left[E/(1\text{eV})\right]^{1/2} \cos 2\delta'(\ell) \tag{46}$$

The problem of analysis consists of extracting the parameters $S(\ell)$ and $\delta'(\ell)$ from the observed cross sections. In Fig. 4 , we show the schematic behavior of the various parts of cross sections as a function of neutron energy for the three different values of the nuclear radius R = 5.0, 7.5, and 10.0 fermi. From this Figure, the following conclusions may be immediately drawn:

1. The $\sigma_p(0)$ remains large over the whole range of neutron energies, whereas the effect of $S(0)$ is felt almost entirely below 200 kev.

2. The $\sigma_p(1)$ contribution is important only above 300 kev, whereas $S(1)$ is significant over all energies above 30 kev.

3. The $\sigma_p(2)$ contribution is always very small; even for R = 10 fermi, at 650 kev the contribution is less than 0.3 barns. Further, because of the small d-wave penetration factor $v(2)$, the $S(2)$ contribution is felt only when $S(2)$ is quite large.

In view of the above observations, the following methods of analysis are immediately suggested in certain specialized energy regions.

Figure 4. Calculated Contribution of Different "Parts" of $< \sigma_t (\ell) >$. Shown here as functions of neutron energy and nuclear radius.

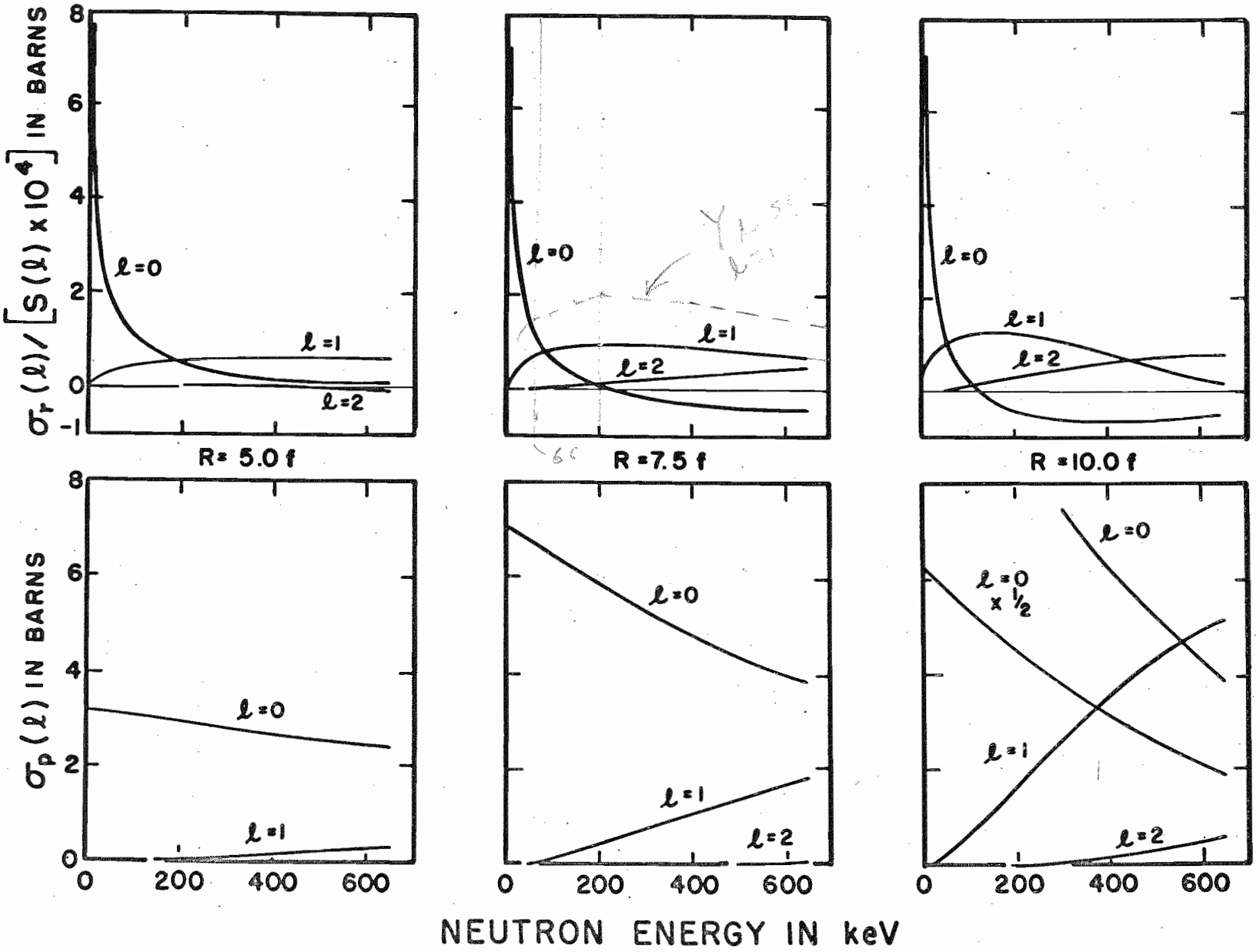
A ≃ 37
A ≃ 125
A ≃ 300
$\sigma_r(\ell) / [S(\ell) \times 10^4]$ IN BARNS
$\sigma_p(\ell)$ IN BARNS
ℓ=0
ℓ=1
ℓ=2
R= 5.0 f
R=7.5 f
R=10.0 f
ℓ=0 x ½
NEUTRON ENERGY IN keV

1. $E_n < 10$ kev. In this energy region, except for very exceptional cases (for example, Nb, for which S(0) is very small and S(1) is very large) it can be safely assumed that the entire cross section is due to $\ell = 0$ neutrons, and as such,

$$< \sigma_t > = 4\pi R'^2 + 2\pi^2 \lambda\!\!\!^{-2} S(0)(E/(1eV))^{1/2} \qquad (47)$$

where

$$\sin\delta'(\ell) = \sin(R'/\lambda\!\!\!^{-}) = R'/\lambda\!\!\!^{-}, \text{ and } v(0) = 1$$

thus

$$S(0) = \text{const. } d< \sigma_t >/d(1/\sqrt{E}) \qquad (48)$$

This method was actually used by Hughes and collaborators (1958) to determine S(0) by measuring thin sample transmission vs. time-of-flight for a large number of nuclei.

It is obvious that R' can be determined by subtracting the resonant contribution from the observed average total cross section, or σ_r for resolved resonances from σ_t. The latter method was used by Seth et al. (1958). Another method for determing R' that is immediately suggested from the observation of Eq. (47) is the following. If D is the average value of spacing for resonances whose average width is $< \Gamma >$ (at an energy where $\Gamma = \Gamma_n$ can be assumed) then it is obvious that for an even-even isotope which has only one spin state for $\ell = 0$ neutrons,

$$< T > = T_p\left[1 - (\Sigma A_{obs}/T_p)/\Delta E\right] \qquad (49)$$

where ΣA_{obs} is the observed area below the potential scattering line for all resonances in the energy interval ΔE.

Or

$$< T > = T_p\left[1 - \frac{< A >}{< \Gamma >}\frac{< \Gamma >}{D}\right] \qquad (50)$$

where $< A > = < A_{obs} > / T_p$. Therefore

$$d \log_e < T > / dn = - \sigma_p + (d/dn) \log_e \left[1 - < A > / < D > \right]$$

$$= - \left[\sigma_p + \frac{< \Gamma >}{< D >} \sum_{m=0}^{\infty} (z^m) \cdot \left(\frac{d}{dn} \right) \left(\frac{< A >}{< \Gamma >} \right) \right] \qquad (51)$$

where

$$Z = < A > / < D > = \frac{< A >}{< \Gamma >} \cdot \frac{< \Gamma >}{< D >}$$

is always less than 1. If one knows the strength function and hence $< \Gamma_n > / < D >$ at the given energy, Z and the derivative are easily obtained from the calculated curves for $< A > / < \Gamma >$. Thus the σ_p is easily obtained. As is well known, as $n\sigma_o$ increases, the derivative in the second term becomes smaller (for δ = finite, it even becomes zero). Assuming it to be very small for large enough $n\sigma_o$, Seth (1958) obtained estimates of σ_p and hence R' for a number of nuclei.

The methods described above suffer from three restrictions:

a) They cannot be conveniently used for energies for which the resonance-potential interference becomes important.

b) They cannot be conveniently used for nuclei for which Doppler-broadening of resonances is important.

c) They cannot easily be extended to higher angular momenta*, or to cases when more than one angular momentum contributes to the observed cross section.

---

*R. G. Thomas (1955) developed an interesting formalism in which average transmission was obtained directly in terms of the R-Matrix theory parameters. The method is substantially equivalent to the considerations described above and therefore suffers from the same disadvantages. It was actually used for the determination of strength functions by Darden (1955).

2. For $E_n < 200$ kev. If somehow we possess the knowledge that for certain nuclei only $\ell = 0$ interactions are important, even then the methods outlined (for the energy region $E_n < 10$ kev) cannot be used to obtain the s-wave parameters $S(0)$ and R' from cross sections in the region 10 - 200 kev. The reasons for this are twofold: $\sigma_p(0)$ can no longer be assumed constant, and interference between potential and resonance scattering becomes important. Marshak and Newson (1957) attempted to tackle this problem in a substantially different manner. Eq. (50) can be rewritten as

$$\frac{<\Gamma>}{<D>} = T_p^{-1}\left[\text{Total area below } T_p \text{ in } \Delta E\right]/(\Delta E < A >/< \Gamma >) \qquad (52)$$

To the first order, the effect of interference between resonance and potential scattering was taken into account by Marshak and Newson (1957) by writing

$$(A/\Gamma) = \pi z e^{-z}[I_o(z) + I_1(z)][1 - (z/2)\tan^2 2\delta'(0)] \qquad (53)$$

where $z = n\sigma_o/2$. They assumed values of R', or equivalently $\delta'(0)$, calculated T_p and $< A >/< \Gamma >$ from equations above and used Eq. (52) to obtain $< \Gamma >/< D >$. They used transmission measurements using two substantially different sample thicknesses to provide consistency check to their results. Marshak and Newson (1957) were only partially successful in their attempt since they did not take account of the difference between R' and R, and assumed $R' = 1.45 a^{1/3}$ fermi, that is, equal to the hard-sphere value. In a subsequent revision of their work, Seth (1958) replaced the A/Γ values of Eq. (53) by more exact values obtained by numerical integration (Seth, 1959a) and analyzed the same two sample thickness data treating both $S(0)$ and R' as free parameters. Unfortunately, the results of the reanalysis by Seth (1958) are also questionable for the following reasons:

a) As mentioned in Section C of Chapter II, if one uses the low energy definition of strength function, one obtains a term in the expression for $< \sigma_t >$ that is proportional to $[S(0)]^2$. The results are thus only correct in the low energy definition of S(0), which is not proper for energy region covered by the Marshak and Newson (1957) data.

b) The reanalysis did not take into account the Doppler effect or the distribution function effect.

c) No allowance for the possible existance of a finite contribution due to p-wave was made.

Having described the previously-used methods for the analysis of average total neutron cross sections, we now describe the methods used in the analysis of experiments reported in this dissertation. This method was developed in the last six years by Seth et al. (1964) and has proven remarkably successful in the extraction of optical model parameters when contributions due to more than one angular momentum are important. In principle, the method is extremely general, although in its application a number of approximations are introduced. Some of these are approximations made strictly for the purpose of reducing the mathematical work, some present the lack in our present knowledge of the behavior of certain parameters, while others are essential to the method of analysis. In its completely general form, the expression for the average transmission due to a mixture of isotopes (labeled by subscript i) may be written as

$$< T > = \prod_i \prod_\ell \prod_J T_p(i\ell J) \quad < T_r(i\ell J) > \qquad (54)$$

where

$$< T_r(i\ell J) > = \left[1 - \frac{< A(i\ell J) >}{< \Gamma(i\ell J) >} \frac{\Gamma(i\ell J)}{\Gamma_n(i\ell J)} \cdot S(i\ell J)v(i\ell J)(E/1)^{1/2}\right] \qquad (55)$$

and

$$T_p(i\ell J) = \exp\left[- n_i\sigma_o(i\ell J) \cdot \sin^2\delta'(i\ell J)\right] \qquad (56)$$

In the above expression, $< A >/< \Gamma >$ is a function of

(1) $n_i\sigma_{oi}(J) \frac{\Gamma_n(i\ell J)}{\Gamma(i\ell J)}$

(2) $\delta'(i\ell J)$

(3) $t(i\ell J) = \left[\frac{\Delta(i)}{\Gamma(i\ell J)}\right]^2 = \left[\frac{\Delta(i)}{S(i\ell J)D(i\ell J)v(i\ell J)(E/1)^{1/2}}\right]^2$

It is obvious that while for a monoisotopic transmission sample the products over the different isotopes i can be dropped, and that for even-even targets, for the $\ell = 0$ case, only one value of J, namely $J = 1/2$, is involved, in general Eq. (54) is much too complicated and must be simplified considerably before being used. We now argue the case for a number of simplifications.

1. The J dependence of neutron strength functions or phase shifts for potential scattering is far from being known. There is no doubt that such a dependence must exist. For $\ell = 0$, empirical evidence has been presented (Seth, 1961; Firk, 1963; Julien, 1965) that a J dependence might exist. However, we must consider the question of the possible J dependence of s-wave strength function as essentially unsettled so far. The presence of the spin-orbit coupling in the optical model potential insures that $S(\ell)$ must be different for the two cases $\ell \pm 1/2$, for $\ell > 1$. However, this dependence cannot be conveniently introduced in the analysis. Firstly the values of $S(1)$ for

$\ell \pm 1/2$ differ by varying amounts for different nuclei, and secondly the difference can only be obtained after obtaining a theoretical optical model fit to the observed $S(l)$. We have therefore chosen to neglect these J dependent differences in $S(\ell)$ and $\delta'(\ell)$ rather than make our results depend on the very model which we are attempting to verify.

2. In our method of analysis we assume that $(\Gamma_n/\Gamma) \sim 1$. For most nuclei for energies above 20 kev this is a fair approximation on an average, i.e., $<\Gamma_n>/<\Gamma> \sim 1$. However, for the very narrowest s-wave resonances and for many p-wave resonances Γ_n may be comparable to Γ_γ. We have verified that for s-wave resonances the effect due to narrow resonances is negligibly small (see Appendix 3, for details). For p-wave resonances the justification is far weaker, even though their major contribution comes only in regions $E_n > 100$ kev. Having no direct knowledge of p-wave Γ_γ, we are essentially forced into this assumption. One fact reduces the error due to this approximation. For small values of $n\sigma_o g\Gamma_n/\Gamma$, the curve $<A/\Gamma>$ versus $n\sigma_o g\Gamma_n/\Gamma$ is nearly linear. Thus the quantity (A/Γ) determined for a value of $n\sigma_o g(J)$ is substantially equal to the correct quantity $(A/\Gamma)(\Gamma/\Gamma_n)$ determined for the corresponding $n\sigma_o g\Gamma_n/\Gamma$, and the average transmission remains unaffected.

3. For a sample containing a natural mixture of different isotopes, it may be assumed that the parameters $S(\ell)$ and $\delta'(\ell)$ are independent of the isotope i. This approximation is generally true since the isotopes are usually close in their values of atomic weight, and the optical model parameters (by definition) are expected to vary smoothly with atomic weight. The worst error caused by this approximation may be expected for nuclei which lie on

the rapidly rising or rapidly falling part of the strength function peaks. In all cases, however, a distinction between even-even and odd A isotopes must be made because of the different g(J) values involved, and also because of the different values of t required due to the rather large differences between the spacings D(J) for odd and even isotopes.

When all the simplifications mentioned above are made, equations (54), (55), and (56) reduce to the following:

$$< T > = \prod_{\ell} T_p(\ell) < T_r(\ell) > \tag{57}$$

where

$$\begin{aligned} T_p(\ell) &= \exp\left[- n4\pi\lambda\!\!\!^{-2}(2\ell + 1)\sin^2\delta'(\ell) \right] \\ < T_r(\ell) > &= \pi_J \left[1 - < A >/< \Gamma >_{\ell J} S(\ell)v(\ell)(E/1)^{1/2} \right] \end{aligned} \tag{58}$$

where the subscript i now refers only to the subdivision between odd and even isotopes. In the region from 0 to 650 kev, from Fig. 4 it is obvious that we need only consider ℓ = 0, 1, and 2 neutron interactions. Thus the average transmission involves six unknowns, $S(\ell)$ and $\delta'(\ell)$ for ℓ = 0, 1, and 2. Besides these, the knowledge of certain auxiliary quantities is also required. These are

1. D(J). This is required in order to obtain the value of the Doppler parameter t. As will be shown later, the accuracy in the value of D(J) desired is far from critical, and an estimate accurate to within a factor of two suffices for nearly all purposes.

2. $v(\ell)$. It can easily be shown that the correct value of $v(\ell)$ to be used in Eq. (58) must itself be obtained from a realistic nuclear model, such as the optical model. However, since the role of $v(\ell)$ is strictly in the

definition of the quantity $S(\ell)$, we may very well use the much more convenient hard-sphere value of $v(\ell)$. We must however remember that the optical model prediction of $S(\ell)$ must also be obtained by the equation $S(\ell) = (\Gamma/D)/v(\ell)$(hard sphere) and not by $S(\ell) = (\Gamma/D)/v(\ell)$(optical model). To a certain extent the variation of $v(\ell)$ with E depends on the nuclear radius assumed. We have assumed $R = 1.45\, A^{1/3}$ since the best square-well optical model fits find this radius useful.

Of the six parameters involved in $< T >$, the least important is $\delta'(2)$. Its contribution to $< T >$ is so small that it may easily be replaced by $\delta(2)$, the hard-sphere phase shift. As will be seen later, it is impossible to obtain unambiguously the values of the remaining five parameters by searching for a best fit to the observed transmission, or equivalently, the apparent cross section

$$\bar{\sigma}_t = - (1/n)\log_e < T >. \qquad (59)$$

Because of the number of approximations involved in Eq. (58), a number of equivalent sets of values of the five parameters can generally be obtained, all of which fit the experimental data equally well. This fact poses the basic problem for the method of analysis. The method due to Seth (1960) solved this problem by the observation that for thick samples the quantity A/Γ is a non-linear function of the sample thickness n, and is extremely sensitive to the value of the potential phase shift $\delta'(\ell)$ (Seth, 1959a) Since at a given energy the magnitude of the s- and p-wave potential scattering is very different, the behavior of the quantity A/Γ as a function of sample thickness for $\ell = 0$ neutrons is expected to be entirely different from that due to $\ell = 1$ neutrons. In particular, at a given energy the

quantity A/Γ for s-wave resonances may go from a maximum positive through a zero to a (large) negative value, while at the same energy the p-wave A/Γ values all remain positive and vary linearly with n, as in the thin-sample approximation. As a result of this property, it is possible to decompose the contributions due to $\ell = 0$ and $\ell = 1$ neutron interactions by measuring the apparent cross sections with transmission samples of different thicknesses. In principle, the method can similarly be extended to differentiate between p- and d-wave neutron contributions, but the sample thicknesses required to do so are so large that experimental effects, such as multiple scattering and the very small values of transmission make the method unfeasible. However, Seth et al. (1960) found that this effect does indeed provide an extremely potent technique in differentiating between the s- and p-wave components of the cross section. As already mentioned in Chapter III, we generally measured the apparent cross sections for three different sample thicknesses. The first sample thickness was chosen to give as close to the true cross section as could be obtained consistent with the desired statistical accuracy, the second one chosen to quench the s-wave contribution as much as possible, i.e., make $A/\Gamma \sim 0$ for s-wave resonances as nearly as possible, and the third was chosen to enhance the p-wave contribution consistent with the considerations of multiple scattering.

Apart from the simplifications already mentioned, a number of other assumptions were also made for the purpose of analysis of the apparent cross sections measured with different sample thicknesses.

1. It was assumed that the parameters $S(\ell)$ and $\delta'(\ell)$ are energy independent. Table 2, derived from the theoretical optical model calculations of

Table 2

Typical Energy Dependence of Average Optical Model Parameters From Buck and Perey (Private Communication to K. K. Seth, 1963)

Parameter	E_n(kev) a	30	50	60	100	140	160	180	210	230
S(0)	10	0.87	5.25	4.0	0.9	3.50	5.70	2.75	1.30	1.05
	40	0.85	4.95	3.85	0.92	3.30	5.25	2.62	1.28	1.03
R'	10	4.15	3.3	6.7	6.2	4.5	7.6	9.0	8.7	8.4
	40	4.02	3.2	6.3	6.1	4.2	6.9	8.5	8.3	8.1
S(1)	10	5.95	1.23	0.95	6.30	1.45	0.97	0.98	2.06	5.05
	40	6.05	1.22	0.95	6.20	1.38	0.98	0.98	2.27	5.15
	100	5.85	1.25	0.97	5.80	1.30	0.96	0.99	2.40	5.00

Perey and Buck (1962), indicates the general validity of this statement. This assumption is poorest near strength function peaks and best in valleys. In all cases, however, the predicted energy variation is much less than 5% per 100 kev, and is thus well within the experimental errors.*

2. Since values of $D(J)$ are known only for s-wave resonances, it was assumed that for all other angular momenta $D(J)$ could be obtained by using the relation that $D(J) \propto (2J + 1)^{-1}$.

3. For $\ell = 1$ and $\ell = 2$ neutrons, Γ is much smaller than for s-wave resonances. Thus the quantity Γ_n/Γ may be much less than unity, and hence the Doppler parameter t may be much larger than for s-wave resonances. Both of these effects combine with the smallness of $v(\ell)$ to make

$$< T_r(\ell) > \exp(- n(\sigma_r(\ell)), \ \ell = 1, 2 \qquad (60)$$

and as such, the complicated expression (58) need not be evaluated for these cases. Indeed, the expression Eq. (58) was never used for the p-wave contribution, instead the thin-sample approximation was used for both p-wave and d-wave resonance contributions. Table 3 demonstrates that the error introduced in the p-wave cross section by using the thin-sample approximation is negligible.

Our method of analysis in actual practice involved three distinct steps. We discuss these below.

1. Reduction of data: The elementary reduction of data and the calculation of errors for the measured cross sections have already been described

---

*It is well worth observing here that Seth et al. (1964) did find definite indications of energy variations of the p-wave strength functions near the sharp maximum around A = 93.

Table 3

Error Introduced in (A/Γ) by Use of Thin Sample Approximation in the worst p-wave case

E_n(kev)*	v(1)	$n\sigma_o$	$\delta(1)$	$\left[\frac{(A/\Gamma)(\text{thin sample approx.})}{(A/\Gamma)(t = 512)} - 1\right]\cdot 100\%$
52	0.13	2.5	0.02	3
85	0.24	1.5	0.06	2
221	0.48	0.6	0.2	0
441	0.65	0.3	0.4	0

*n = 0.1 atoms/barn, R ~ 8 fermi, $S(1) = 6 \times 10^{-4}$, $\langle g(J) \rangle = 1/2$ and $\langle D \rangle \sim 10$ eV, were assumed in these calculations. The above parameters imply $(\Gamma_n/\Gamma) \sim 1$, and t = 512.

in Chapter III. The program for Data Reduction (PROD) and typical input and output are given in Appendices 4 and 5.

2. Analysis of thin-sample cross sections for preliminary optical model parameter selection: In this step of preliminary analysis, it is assumed that the observed thin-sample cross sections are very close to the true $< \sigma_t >$, i.e., they can be represented correctly by equations (45) and (46), with the summation over ℓ extending over $\ell = 0$, 1, and 2, for energies up to 650 kev. As already mentioned, $\delta'(2)/\delta(2)$ can be considered to be very close to unity, and therefore only five parameters need to be adjusted to calculate the total cross sections for the thin sample. It would appear that a five dimensional, least-squares fitting program, in which the five parameters are allowed to vary over the physical region, is required to select the correct parameters. In actual practice, however, the mathematically least-squares solution has no greater validity than the many other combinations of parameters which fit the data with a RMS error which is well within the range of experimental errors in the measured cross sections. All such solutions are, for our purposes, equivalent, and therefore must be examined equally seriously. A computer program (POPS) conforming to this philosophy was therefore written. Its details are presented in Appendices 4 and 5. During the first iteration, a coarse grid size and a wide range of each of the five parameters was given to the program for search of acceptable solutions. Successively narrower ranges and finer grids were then used. As many as 100,000 combinations of parameters were tried by this program, and out of these 50 to 80 were usually found to meet the criterion of fitting the data well within the specified maximum RMS error. (Part of such output for Sb is shown in Appendix 4).

Surprisingly enough, the frequency distribution for individual parameters, as they occur in the acceptable combinations, usually had maxima for values which were very close to the final values of the parameters (obtained from the complete area analysis of the three sample thickness data). For example, the POPS analysis of the thin sample data on Sb yielded the frequency distribution shown in Fig. 5. From these distributions, the best fit parameters suggested are $S(0) = 0.45$ (fixed value), $S(1) = 2.3 \pm 1.0$, $S(2) = 1.0 \pm 1.0$, $\delta'(0)/\delta(0) = 0.8 \pm 0.1$, $\delta'(1)/\delta(1) = 0.7 \pm 0.5$. The final result for Sb, based on thin and thick sample analysis, is (see Table 5) $S(0) = 0.45 \pm 0.20$, $S(1) = 2.0 \pm 0.5$, $S(2) = 1.5 \pm 0.7$, $\delta'(0)/\delta(0) = 0.8 \pm 0.05$, $\delta'(1)/\delta(1) = 1.0 \pm 0.18$*.

3. Area analysis of thick sample data for final optical model parameter selection: The analysis described in the preceeding section is meant to provide the starting point in the search for the best optical model parameters using the area analysis methods described earlier in this Chapter. For this purpose, the cross sections obtained from all three sample thicknesses are fitted. As already mentioned the area method needs to be applied only to s-wave contributions. A program was therefore written to compute p-wave and d-wave cross sections by the thin sample approximation, and s-wave cross sections by the area method. The sum $\Sigma < \sigma_t(\ell) >$ was compared with experimentally measured total cross sections. This program (TOPS) is described in Appendices 4 and 5.

---

*All numerical strength function values in this dissertation are given in units of 10^{-4}.

Figure 5. Typical Frequency Distributions for Acceptable Parameters Based on POPS Analysis.The histograms are from actual analysis of Sb data.

ANTIMONY

N = 0.0334 atoms/barn

S(0) = 0.45 (fixed)

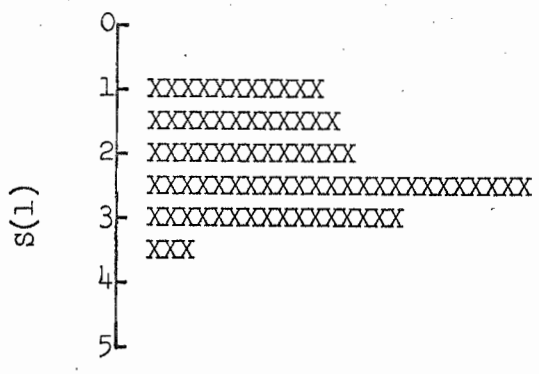

S(1) = 2.3 ± 1.0

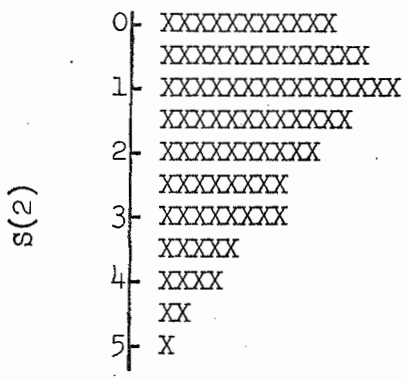

S(2) = 1.0 ± 1.0

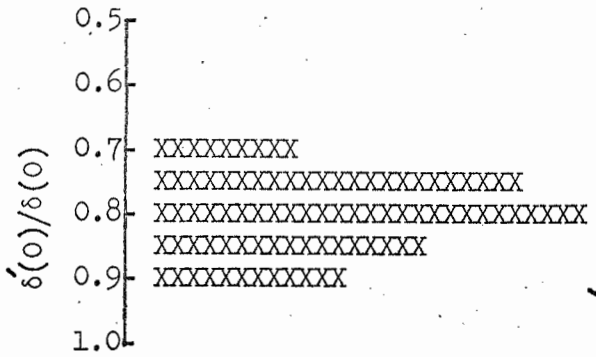

δ′(0)/δ(0) = 0.8 ± 0.1

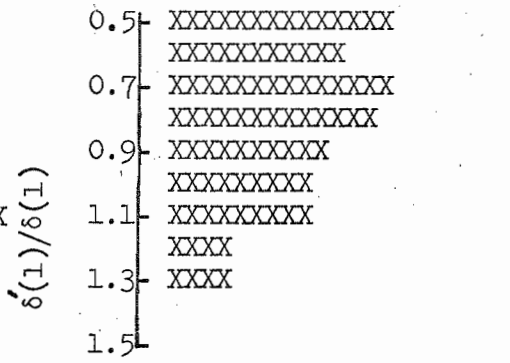

δ′(1)/δ(1) = 0.7 ± 0.5